

Polarity Reversal in PEM Fuel Cells by Fuel Starvation

M. A. Travassos , C. M. Rangel

LNEG - Laboratório Nacional de Energia e Geologia, Fuel Cells and Hydrogen Unit,
 Paço do Lumiar, 22 1649-038 Lisboa Portugal
carmen.rangel@lneg.pt; antonia.travassos@lneg.pt

Abstract

In this work, the degradation caused by polarity reversal by fuel starvation of a 16 MEA – low power fuel cell is reported. Measuring of the potential of individual cells, while on load, was found instrumental in the location of affected cells which revealed very low or even negative potential. Electrochemical impedance spectroscopy in-situ gave insight on the increase in resistance and diffusion processes. Ex-situ analysis of MEA after irreversible degradation by fuel starvation gave as a result delamination of catalyst layers with impacts on fuel cell performance such as development of flooded areas by the pockets created increasing the resistance of reactant transport to the catalyst sites. Striking and thickness variation of the anode layer as well as carbon corrosion were found. The proton exchange membrane is also affected by fluoride depletion.

Keywords: polarity reversal, fuel starvation, PEM degradation, AC impedance characteristic, morphological defects.

1 Introduction

Durability criteria for fuel cells require a minimum lifetime of 40000 hours for stationary applications and 5000 hours for automotive applications [1, 2]. Fuel cells are prone to chemical, mechanical or thermal degradation that lead to a voltage/performance decline and lifetime reduction.

The major morphological defects identified on the membrane-electrode assembly (MEA) are cracking, delamination, catalyst clusters, and thickness variations, due to manufacturing or operating conditions.

The baseline degradation is irreversible and unavoidable, due to long-term material degradation in the context of load cycling and/or the influence of the variation of operating conditions such as temperature and humidity on cell performance. PEMFC lifetime, for instance can be reduced by degradation of the MEA, Pt dissolution and/or agglomeration or carbon corrosion promoted by different operation conditions such as MEA contamination by impurities and power or thermal cycling. On the other hand, sudden degradation may occur by detrimental operating conditions such as reactant starvation, mostly fuel starvation [2].

In this work, polarity reversal caused by fuel starvation of a 16 MEA low power fuel cell is reported associated to an application in emergency exit lighting. Morphological defects detected by SEM/EDS were linked to delamination and thickness variation. AC impedance spectroscopy allowed characterization of transport losses, and evaluation of ohmic and charge transfer resistances.

2 Experimental

In this work an emergency exit light which integrated a NiCd battery of 3.6V with a storage capacity of 4Ah, was substituted by a low power PEM fuel cell supplied with hydrogen.

Emergency exit lightening is usually associated to big capacity batteries or a modest autonomy. In this case the system with hydrogen fuel cells can extend the system autonomy and give others advantage such as easier logistic when compared to battery maintenance.

Figure 1 shows the schematic drawing of the PEM fuel cell (A) used in this work as well as the circuit implemented using a hydrogen storage system constituted by a metallic hydride (B).

The fuel cell, SRE technology, had a nominal power of 15 W (16 cells) and the metallic hydride small reactor had a capacity for 50 NL H₂.

The MEA morphological aspects, after dismantling of the cell, were observed by SEM/EDS.

Elemental mapping was implemented for MEA cross section analysis in order to register the elemental chemical distribution of P, F and S. A SEM.

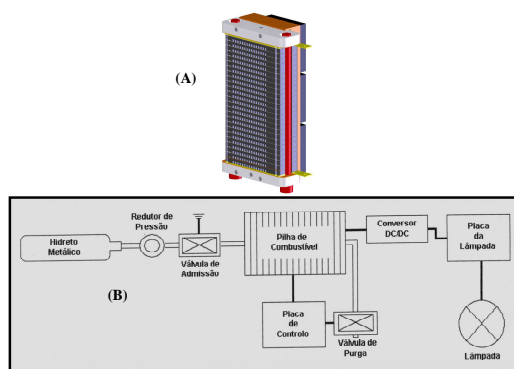


Fig. 1 PEMFC, and an electrical circuit feeding an emergency exit lightening with a H₂ fuel cell (A). Metallic hydrate (B) as hydrogen storage system.

The PEM fuel cell performance was studied allowing evaluation of the fuel cell autonomy.

While on loading, the fuel cell was operated during one hour daily. Measurements of cell potential took place every 15 minutes. The potential was registered for every of the 16 cells integrating the stack.

At the end of the mentioned tests the electrochemical behaviour of the cell was evaluated by EIS - Electrochemical Impedance Spectroscopy, allowing the separation of the cathode and the electrolyte.

Electrochemical impedance spectroscopy is being widely used as a diagnosis technique for proton exchange membrane (PEM) fuel cells degradation studies. In this case a two-electrode configuration is used; the anode provides two functions as counter and reference electrode. The drawback of the two-electrode measurements is the impossibility of evaluation the participation of both individual electrodes, nevertheless, in fuel cell operation, the anode polarization was considered negligible against cathode polarization [3].

A Frequency response analyzer from Solartron Model 1250 was used connected to an Electrochemical interface also from Solartron Model 1286. The range of frequencies covered spans from 45000 Hz to 0.01Hz.

3 Results

While on load, emergency light switched-on, the cell potential values were individually measured showing a dependency on cell position in the stack. Lower values are reported for the farthest cells from hydrogen entry. The potentials values vary from 0.653V down to 0.492V, figure 2, with the lowest values associated to cells 15 and 16.

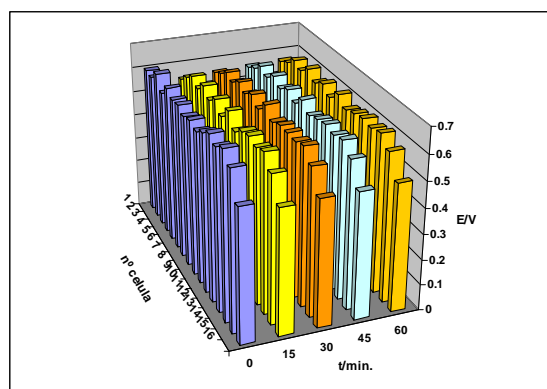


Fig. 2 Cell potential *versus* time for a 15 W fuel cell stack of 16 cells. Data are referred to one hour operation, with measurements every 15 minutes.

Data registered for 3 consecutive days were very similar, with a slight increase in potential values.

EIS spectra were taken for the system after one hour operation, typical results are shown in figure 3. Two semicircles are evident in the Nyquist diagram, figure 3(a), with two time constants well separated in the frequency domain; see Bode plot in figure 3(b).

In the fuel cell, the proton conducting membrane separates the anode from the cathode compartment where electrocatalytic oxidation of H₂ and reduction of O₂ occur, respectively. The selected equivalent circuit for the anode and cathode are described by two RC circuits, and an ohmic resistance in series accounts for the presence of the

polymeric membrane, as shown in the inset of figure 3 (a).

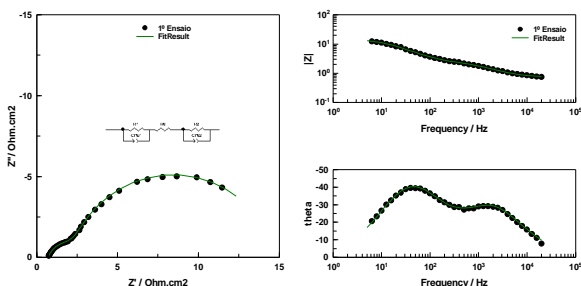


Fig. 3 Impedance spectra for a Low power 16 cell stack after one hour operation. Nyquist diagram and equivalent electrical circuit (a); Bode diagram (b). the selected equivalent circuit for fitting is also shown in figure 3a).

Even though the cathode resistance did not significantly change with time of operation, the electrolyte resistance (R_0) increase from $0.74\Omega\text{cm}^2$ to $0.81\Omega\text{cm}^2$ and this was associated with membrane conductivity and hydration. The value of 45° for the phase angle evident at low frequencies in the Bode diagram confirms limitation by diffusional control, figure 3(b).

With continuous operation using a reduced hydrogen flow an inversion of polarity was observed in the 16th cell of the stack, evident in the potential vs time plot in figure 4, as a result of insufficient hydrogen to reach the last cells.

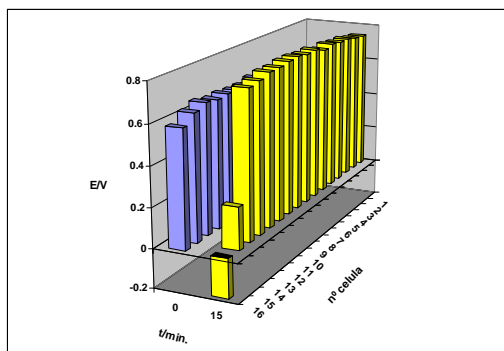


Fig. 4 Cell potential of a 16 cell low power PEM fuel cell versus working time showing polarity reversal in cell 16 and potential below 0.2 V in cell 15.

Figure 5 shows the impedance spectrum (Nyquist diagram) corresponding to the same operating conditions depicted in figure 5. The spectrum reveals a dissimilar behaviour related the previous EIS data with a higher electrolyte resistance, $R_0=2.50\Omega\text{cm}^2$, and a semicircle at middle frequencies ($R_2=22.01\Omega\text{cm}^2$ - $CPE_2=15.66\mu\text{F.cm}^2$), slightly depressed due to the porosity of the electrodes. The presence of an inductive loop at low frequencies, pointed to an adsorption process.

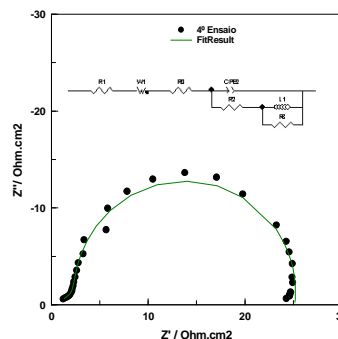


Fig. 5 Nyquist diagram and equivalent electrical circuit after potential reversal.

The degradation level of the fuel cell was evaluated by measuring the potential with time every 30 minutes, figure 6, being more accentuated the difference between the potential of the middle cells in comparison with the peripheral cells that presented lowers values, particularly the 16th cell.

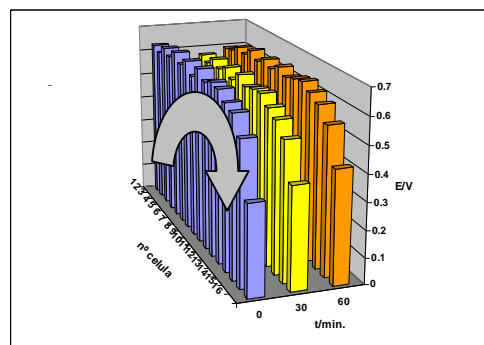
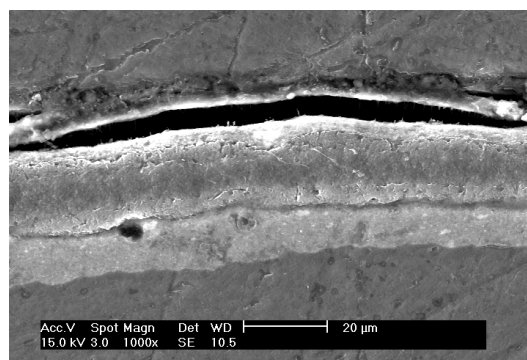


Fig. 6 Cell potential of a 16 cell low power PEM fuel cell after polarity reversal, when the full flux of hydrogen has been replenished.

Once the phenomenon is made irreversible, the cell was dismantled in order to observe the degradation of the MEA.

The cells were observed under the SEM after cross section mounting. Images revealed the presence of morphological defects associated to fuel starvation.

The SEM observation of the cross sections were accompanied by EDS mapping for Pt, S and F, corresponding to the 16th cell. Results are represented in figure 7. The images show delamination at the anode and a striking difference of thickness when compared to the cathode catalyst layer (C), see table 1.



(a)

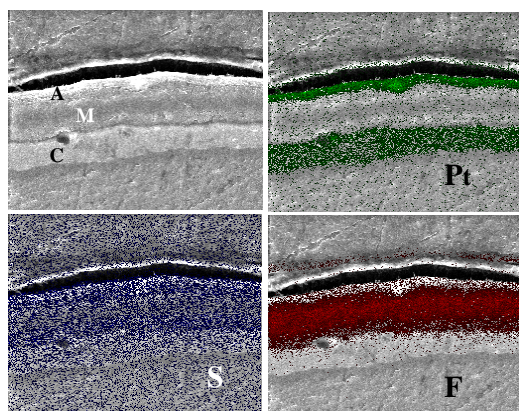


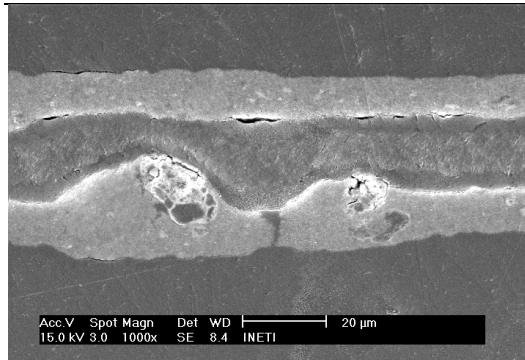
Fig. 7 SEM image of cross section of the MEA of the 16th cell showing delamination (a) and the results of elemental mapping for the Pt, S and F. A= anode; C= cathode and M= membrane (b)

Table 1 Anode, cathode and membrane average thicknesses of different cells in the tested PEM stack.

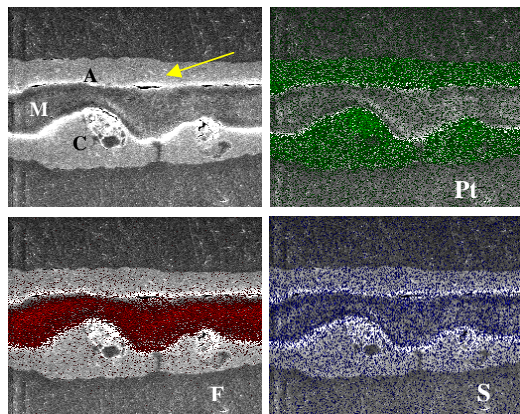
Sample	Anode Thickness µm	Cathode Thickness µm	Membrane Thickness µm
Cell 1	10.02	9.79	14.21
Cell 9	10.63	9.98	18.63
Cell 16	4.86	12.96	17.74

The following observations and implications were made:

- The 16th cell presents the lower performance and also the greater reduction on the anode thickness compared with the other cells, this is thought to be due to the consequences of polarity reversal.
- The thickness variations can promote variable resistance through the MEAs. Thicker areas of the catalyst layer will have higher electronic resistance, while thicker electrolyte segments will have increased ionic resistance. For thinner areas, the opposite will be true.
- The thinner areas of the ionomer coupled with a thicker catalyst layer will be more susceptible to degradation by heat.
- Since the mechanical strength of the MEA comes partially from the electrolyte membrane, areas where the electrolyte is deep-set by the catalyst layer may be mechanically weak and thus may tear easily with tension. This may cause problems with pressure differentials and mechanical stress during thermal and hydration cycles [1].
- The first cell presents also delamination with separation between catalyst layer (anode A) and polymer membrane electrolyte (M), as pointed in figure 8.
- The delamination can also increase resistance in MEA. The separation of the catalyst layer from the electrolyte reduces also the total contact area between the two layers. Hence, the contact resistance between the materials will increase, the protons will have a longer path to travel to catalyst sites, and the water barrier will be more resistive to proton conduction than pure electrolyte.
- Some features observed are adjudicated to carbon corrosion, figure 8.
- Fluoride depletion in the membrane is suggested near the borderline with the catalyst layer.
- On the other hand, the cells located in the middle of the stack (cell 9) are more homogeneous and show no delamination, see figure 9.



(a)



(b)

Fig. 8 SEM image of the 1th cell in cross section (a) and EDAX mapping for the Pt, S and F elements. A =anode; C=cathode and M= membrane (b). Delamination is and carbon corrosion is indicated.

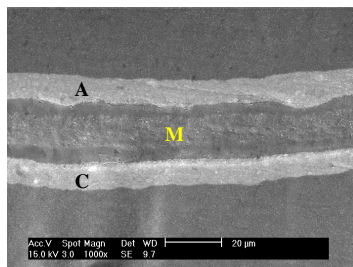


Fig. 9 SEM image of the 9th cell in cross section. A anode, C cathode and M membrane.

4 Final Remarks

The reduced flow of hydrogen in the fuel stack caused the reversal of polarity in one of the cells with consequent deterioration of the properties of the stack.

Morphological aspects reveal deterioration of peripheral cells with emergence of delamination and varying the thickness of the catalyst layers anodic and cathodic. Furthermore, carbon corrosion and fluoride depletion in the membrane are suggested.

5 References

- [1] S. Kundu, M.W. Fowler, L.C. Simon, S. Grot, Morphological features in fuel cell membrane electrode assemblies *J. of Power Sources*, 157 (2006) 650-656;
- [2] N. Yousfi-Steiner, Ph. Moçotéguy, and all, A review on polymer electrolyte membrane fuel cell catalyst degradation and starvation issues: Causes, consequences and diagnostic for mitigation, *J. of Power Sources*, 194 (2009) 130-145;
- [3] Jinfeng Wu, Haijiang Wang, and all, Diagnostic tools in PEM fuel cell research: Part I Electrochemical techniques, *Int. J. of Hydrogen Energy*, 33, (2008) 1735-1746